IOP Publishing | Institute of Physics and Engineering in Medicine Physics in Medicine & Biology

Phys. Med. Biol. **59** (2014) 6031–6042 doi:10.1088/0031-9155/59/20/6031

Electroporation in cancer therapy without insertion of electrodes

John Lekner

MacDiarmid Institute and School of Chemical and Physical Sciences, Victoria University of Wellington, PO Box 600, Wellington, New Zealand

E-mail: john.lekner@vuw.ac.nz

Received 20 July 2014, revised 18 August 2014
Accepted for publication 19 August 2014
Published 17 September 2014

Abstract

Electroporation in cancer therapy in which elongated micron-sized conductors are used to enhance an externally applied electric field is investigated. Such field enhancement was previously used in carbon and boron nitride nanotube electropermeabilization. It is envisaged that the micro-conductors would be injected together with therapeutic drugs into tumorous regions, and a pulsed or alternating external field would be applied. Amplification of this external electric field at the pointed ends of the elongated micro-conductors would then give (locally) a field sufficiently large to cause electroporation. The torque of the electric field on the polarized micro-conductors will tend to align them with the field, giving the configuration of maximum field enhancement at their ends. Brownian (thermal) motion will disrupt this alignment. We give an analysis of field enhancement, torque, and thermal motion for micro-conductors of prolate spheroidal shape, and estimate the range of their size for use in human tissue.

Keywords: electroporation, cancer, field enhancement

(Some figures may appear in colour only in the online journal)

1. Introduction

The purpose of this note is to analyse an electroporation (Weaver and Chimadzhev 1996, Gaynor and Bodger 2006, Vernier *et al* 2006, Pliquett *et al* 2007, Chen *et al* 2008, 2010, Granot *et al* 2009, Ivorra *et al* 2009, Levine and Vernier 2010) method which avoids the need to insert electrodes into tumour regions, as is current practice in cancer treatment (Hoffmann *et al* 1999, Mir 2000, Gothelf *et al* 2003, Sersa *et al* 2008). The required high electric fields are provided by *external* electrodes, and amplified within the patient's body by elongated micro-conductors. The same idea was previously used in carbon and boron nitride nanotube electropermeabilization (Smythe 1950, Rojas-Chapana *et al* 2004, Raffa *et al* 2009, 2010a,

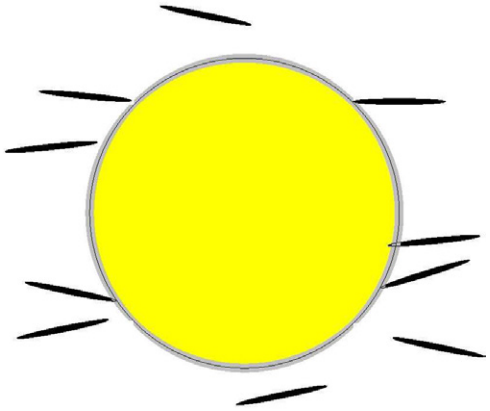

Figure 1. A cell with spheroidal micro-conductors around it, in an external electric field (horizontal in the figure), which tends to align the micro-conductors. Brownian motion disrupts the orientation slightly. The external field, pulsed or at high frequency, is amplified at the ends of the spheroids, causing pores to form in the cell membrane (electroporation), allowing cancer drugs to enter the cell. For the spheroid aspect ratio shown, the maximum amplification of the field is by a factor of 100.

2010b, 2011). As we shall show, such field enhancement is readily provided: for example, the electric field at the tips of a prolate spheroid aligned with the field is 100 times the supplied external field for aspect ratio (length/width) of about 15.7.

If such a method can be made to work, it would avoid the trauma associated with the insertion of electrodes into the patient, and also the involuntary muscle contractions caused by the application of high voltages internally.

In our numerical examples we shall assume an external field of $2\,\mathrm{MV\,m^{-1}}$ (for instance, 0.4 MV across 20 cm of a patient's torso), reduced by a factor of about 80 inside the aqueous environment of the human body, and amplified at the sharp ends of the injected micro-conductors by the same factor 80 back to $2\,\mathrm{MV\,m^{-1}}$. [In the ideal case of perfect alignment of micro-conductors the example illustrated in figure 1 has field amplification by 100, but that number applies only at the tip of the micro-conductor, and at exact alignment.] These field magnitudes are at the lower end of the range used by Levine and Vernier in their electropore simulations (Levine and Vernier 2010). In section 5, table 1 gives estimates of micro-conductor rotation times and upper and lower limits for the micro-conductor long axis for a wider range of field strengths.

The electric field can be applied as a pulsed or alternating voltage across the body. The pulse duration should be sufficiently short (or the frequency of alternating voltage sufficiently high) so as to not permit substantial drift of ions during one pulse or half-period. The rotational response of the polar water molecules is so fast that the dielectric factor of 80 mentioned in the previous paragraph applies up to the gigahertz range. In section 4 we shall find that there is a constraint on the cumulative time of exposure: for example for $2\,\mathrm{MV\,m^{-1}}$ it needs to about $10\,\mu\mathrm{s}$ or greater than to enable the micro-conductors to orient along the field direction.

We shall discuss field enhancement near elongated spheroidal conductors, their polarizability tensor and its relationship to energy and torque, the rotation of prolate spheroids in a viscous fluid, the Brownian motion which counteracts the tendency of micro-conductors to align with the field, and the optimum size range of the micro-conductors, in sections 2–5 respectively. Figure 1 illustrates the schematics of the proposed electroporation method.

2. Field enhancement by prolate spheroids

The redistribution of charge on a conducting object placed in an external electric field changes the field in its neighbourhood. For example, the field close to a conducting sphere varies from three times the external field to zero. Elongated objects can have much larger field amplification. A representative and calculable shape that can be made as pointed as we wish is the prolate spheroid (Smythe 1950, section 5.281; Morse and Feshbach 1953, p 1284). This is an ellipsoid with semiaxes a, a, c ($c > a$),

$$\frac{x^2}{a^2} + \frac{y^2}{a^2} + \frac{z^2}{c^2} = 1 \tag{1}$$

In prolate spheroidal coordinates (ξ, η), related to the Cartesian coordinates by

$$x^2 + y^2 = (c^2 - a^2)\,(\xi^2 - 1)\,(1 - \eta^2)\,, \quad z = (c^2 - a^2)^{1/2}\,\xi\eta \tag{2}$$

the conductor surface given by (1) corresponds to $\xi = \xi_0$, where

$$\xi_0^2 = c^2 / (c^2 - a^2)\,, \quad \xi_0^{-1} = e = \sqrt{1 - (a/c)^2} \tag{3}$$

(e is the eccentricity). In the longitudinal configuration, when the external electric field points along the long (z) axis of the spheroid, the potential outside the spheroid $\xi = \xi_0$, assuming zero potential on the spheroid, is

$$V = E_0 z \left\{ 1 - \frac{\operatorname{arccoth}\xi - \xi^{-1}}{\operatorname{arccoth}\xi_0 - \xi_0^{-1}} \right\} \tag{4}$$

The electric field at the surface is given by

$$\frac{E}{E_0} = \frac{\eta}{\left[\left(\xi_0^2 - 1\right)\left(\xi_0^2 - \eta^2\right)\right]^{\frac{1}{2}} \left[\,\xi_0 \operatorname{arccoth}\xi_0 - 1\,\right]} \tag{5}$$

At either pole ($z = \pm c$, $\xi = \xi_0$, $\eta = \pm 1$), the field magnification is by the factor

$$\frac{E_p}{E_0} = \frac{1}{\left(\xi_0^2 - 1\right)\left[\,\xi_0 \operatorname{arccoth}\xi_0 - 1\,\right]} \tag{6}$$

The field amplification factor increases without limit as ξ_0 tends to 1 from above (c much larger than a), and the spheroid becomes needle-shaped. In the spherical limit (c tending to a, ξ_0 tending to infinity), the field amplification factor tends to three. Since

$$\operatorname{arccoth}\xi_0 = \tfrac{1}{2}\ln\frac{\xi_0 + 1}{\xi_0 - 1} = \frac{1}{2}\ln\frac{1 + e}{1 - e}, \tag{7}$$

equation (6) can be rewritten as

$$\frac{E_p}{E_0} = \frac{e^3 / (1 - e^2)}{\frac{1}{2}\ln\frac{1+e}{1-e} - e} \tag{8}$$

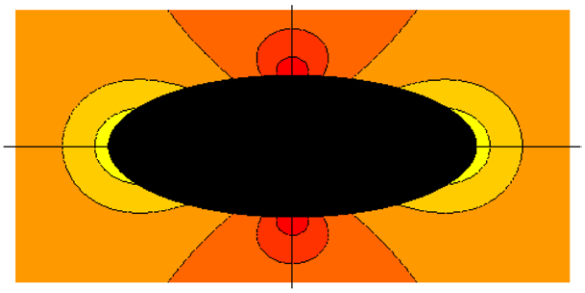

Figure 2. Prolate spheroid, aligned with the external field (horizontal in the figure). The major to minor axis ratio is 13/5; the eccentricity is $e = 12/13$. The field strength contours are in geometric progression, at $E/E_0 = \frac{1}{4}, \frac{1}{2}, 1, 2, 4$.

Figure 2 shows the field magnitude ratio E/E_0 for $\xi_0 = 13/12$, which corresponds to the semiaxis ratio $c/a = 13/5$; in this case the maximum amplification E/E_0 is nearly 8. Note the rapid decrease in the field strength with increasing distance from either pole.

The above calculation is for a spheroid in a homogeneous medium. On the suggestion of a Reviewer, a calculation made in the Appendix and discussed in section 6 reveals that the membrane has a large effect on the electric field in its neighbourhood, despite the fact that it is very thin (about 5 nm) compared to the spheroid dimensions. This is because of the large contrast between the membrane dielectric function and that of the plasma or cytoplasm on either side.

3. The polarizability tensor and the torque

We shall use the polarizability tensor α_{ij} to calculate the torque on a prolate spheroid polarized by an external field. The dipole moment and energy of a conductor in an external field are given by (Landau and Lifshitz 1960, section 2),

$$p_i = \sum_j \alpha_{ij} E_j, \qquad W = -\tfrac{1}{2} \sum_i \sum_j \alpha_{ij} E_i E_j \tag{9}$$

Let us suppose that the spheroid long axis is along the z-axis, and that the external field lies in the zx plane:

$$\mathbf{E}_0 = (E_{0x}, 0, E_{0z}) = E_0(\sin\theta, 0, \cos\theta) \tag{10}$$

The polarizability tensor in this system of coordinates is diagonal:

$$\alpha = \begin{pmatrix} \alpha_{xx} & 0 & 0 \\ 0 & \alpha_{yy} & 0 \\ 0 & 0 & \alpha_{zz} \end{pmatrix} = \begin{pmatrix} \alpha_t & 0 & 0 \\ 0 & \alpha_t & 0 \\ 0 & 0 & \alpha_\ell \end{pmatrix} \tag{11}$$

Thus the longitudinal and transverse components α_ℓ and α_t determine the system energy:

$$W = -\tfrac{1}{2} {E_0}^2 (\alpha_t \sin^2\theta + \alpha_\ell \cos^2\theta) \tag{12}$$

The torque is obtained by differentiation of the energy with respect to the angle θ between the spheroid long axis and the field: its magnitude is

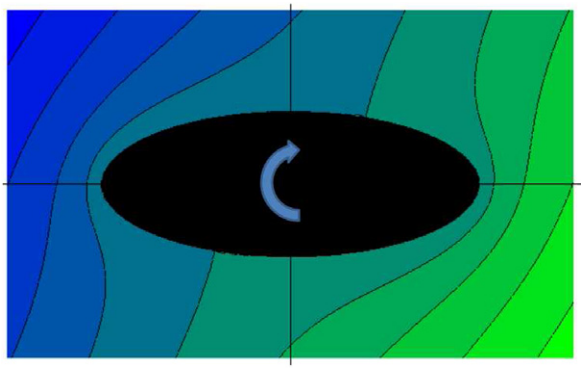

Figure 3. Prolate spheroid inclined at 30° to an external field. The figure shows equipotentials near the spheroid, and the torque on the spheroid (curved arrow).

$$\partial_\theta W = {E_0}^2(\alpha_\ell - \alpha_t)\sin\theta\cos\theta \tag{13}$$

The above formulae apply to a spheroid in free space; in a dielectric medium the electrostatic energy and torque are to be multiplied by the dielectric constant ε (relative to the vacuum) of the medium (Smythe 1950, section 2.11).

The polarizability tensor components for conducting spheroids are known (Landau and Lifshitz 1960, section 4): in terms of the eccentricity e defined by $e^2 = 1 - a^2/c^2 = 1/{\xi_0}^2$,

$$\alpha_\ell = [4\pi\varepsilon_0]\frac{e^3c^3}{3}\left[\frac{1}{2}\ln\left(\frac{1+e}{1-e}\right)-e\right]^{-1}, \quad \alpha_t = [4\pi\varepsilon_0]\frac{2e^3c^3}{3}\left[\frac{e}{1-e^2}-\frac{1}{2}\ln\left(\frac{1+e}{1-e}\right)\right]^{-1} \tag{14}$$

[The factor $4\pi\varepsilon_0 \approx 111\text{pF m}^{-1}$ converts Gaussian units to SI units; ε_0 is the permittivity of free space.] The longitudinal and transverse polarizability components both tend to $[4\pi\varepsilon_0]c^3$ in the spherical limit (eccentricity e tending to zero, a tending to c). For elongated spheroids the longitudinal polarizability dominates, as may be expected. Equations (13) and (14) give the torque: proportional to the square of the field, zero when the spheroid is aligned with the field or perpendicular to the field, maximum at 45° to the field. The torque always acts to align the spheroid with the field. Figure 3 shows equipotentials near a prolate spheroid inclined at 30° to an external field.

Next we shall examine the retarding torque resulting from viscous drag on the spheroid as it tries to align with the field.

4. Rotation of a spheroid in a viscous fluid

We wish to estimate the time that it would take to align a spheroid, moving in a medium of viscosity μ, with the applied electric field. From section 3 we know the aligning torque due to the field; what is the retarding torque due to the viscous drag of the ambient fluid? For slow rotation (we shall verify in section 6 that the Reynolds number is small for cases of interest), the retarding torque is known. Edwardes (1892) treated the slow rotation of ellipsoids (semiaxes *a, b, c*); a multiplicative factor of 5/6 was corrected by Gans (1928). Specialized to the prolate spheroid of semiaxes *a, a, c*, the retarding torque for rotation about a short axis at angular frequency ω is

$$\tau = \frac{16}{3}\pi\mu\omega\, c^3 \frac{e^3(2-e^2)}{\frac{1+e^2}{2}\ln\frac{1+e}{1-e} - e} \tag{15}$$

As a tends to c, the torque tends to the Kirchhoff value $8\pi\mu\omega c^3$ for a sphere rotating about an axis through its centre. Batchelor (1970) considered the more general case of the rotation of slender bodies, with semi-diameters a and $c >> a$. His result (Batchelor 1970, equation (8.10)) is

$$\tau_B = \frac{8}{3}\pi\mu\omega\, c^3 \frac{1}{\ln\frac{2c}{a} - \frac{1}{2}} \tag{16}$$

This result is in agreement with (15) in the limit of e tending to unity from below. The formula (2.4) of Shine and Armstrong (1987) is equivalent to (15), although they refer to Edwardes and not to Gans.

We note that both the driving torque due to the electric field and the retarding torque due to the fluid viscosity are proportional to the volume $(4/3)\pi a^2 c = (4/3)\pi c^3(1-e^2)$ of the spheroid, times form factors which depend on the aspect ratio c/a, or equivalently on the eccentricity e. Thus the rate at which these bodies align with the field will be proportional to the field strength squared, and inversely proportional to the viscosity of the medium, but will not depend on the size of the spheroid, only on its aspect ratio (provided the Reynolds number remains small, as discussed below). The angular rotation rate $\omega(\theta)$, found by equating the driving torque (13) [augmented by the dielectric factor ε] and retarding torque (15), can be written in the form

$$\omega(\theta) = \Omega \sin\theta\cos\theta, \qquad \Omega = \frac{\varepsilon E_0{}^2(\alpha_\ell - \alpha_t)}{\frac{16}{3}\pi\mu\, c^3 \frac{e^3(2-e^2)}{\frac{1+e^2}{2}\ln\frac{1+e}{1-e} - e}} = \frac{[4\pi\varepsilon_0]\,\varepsilon E_0{}^2}{8\pi\mu}F(e) \tag{17}$$

The form factor $F(e)$, defined by (14) and (17), tends to zero for small eccentricity, since the electric torque on a spherical object is zero. For $e \to 1$, the case of interest, the form factor is nearly unity. The behaviour of $F(e)$ over the whole range of eccentricity is shown in figure 4.

The region of validity of (17) is restricted to low Reynolds number, which varies along the spheroids, since the velocity relative to the ambient fluid is proportional to the distance from the axis of rotation. The maximum Reynolds number, at the tip of the spheroid, is of order

$$\frac{\Omega\, c^2\rho}{\mu} = \frac{(4\pi\varepsilon_0)\,\varepsilon E_0{}^2 c^2\rho}{8\pi\mu^2}F(e) \tag{18}$$

When we put in the viscosity of blood at 37 °C, $\mu \approx 35$ milli-dyne s cm^{-2} =3.5 mPa s, the density of blood (ρ) equal to that of water, the dielectric constant likewise that of water ($\varepsilon \approx 80$), the form factor F approximately unity, and an external electric field of 2 volts per micron, we find that the Reynolds number is less than unity provided the spheroids have the longer semi-axis c about 3 microns or smaller.

From $\omega(\theta) = \Omega\sin\theta\cos\theta = -\mathrm{d}\theta/\mathrm{d}t$ (the spheroid rotates under the influence of the field to decrease the angle θ between its long axis and the field), we can estimate the time for rotation of the spheroid from angle θ_0 to angle θ by integration: it is

$$t = \Omega^{-1}\ln[\tan\theta_0/\tan\theta] \tag{19}$$

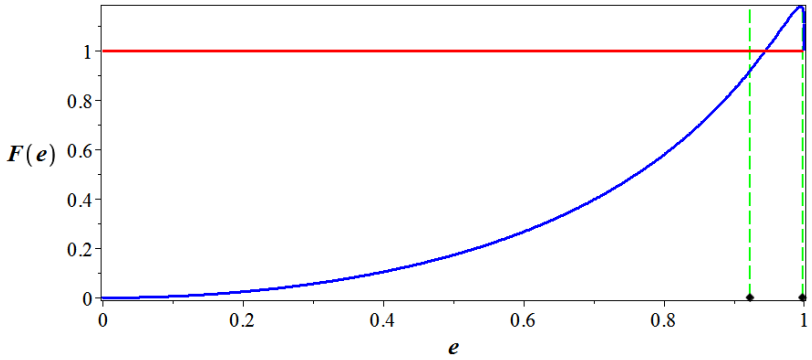

Figure 4. The form factor $F(e)$ defined by (17), versus the eccentricity e. The eccentricities corresponding to figures 2 and 3 ($e = 12/13 \approx 0.923$), and that giving a field magnification of 100 (figure 1, $e \approx 0.998$) are indicated by diamonds and vertical dashed lines.

For example, the time to rotate from $\theta_0 = 60°$ to $\theta = 30°$ will be $\Omega^{-1} \ln[3] \approx 1.1\Omega^{-1}$.

For the parameters just used to estimate the c value for which the Reynolds number is unity, we find Ω^{-1} to be about 2.5 μs. Thus the external field, if pulsed, should have a cumulative 'on' time of 10 μs or more. Alternating fields will also align the spheroids, since the torque is proportional to the square of the field and always acts to align the spheroid long axis with the field. A similar or longer 'on' time is required to align the micro-conductors.

5. Thermal motion, and the optimum size of spheroidal micro-electrodes

What would be the optimum size of the elongated conductors injected together with anti-cancer drugs? If large they will be unnecessarily invasive, and will not orient easily in the patient's body tissue; also the formulae for viscous drag we gave apply only if the long semiaxis is no more than a few microns, as we saw in the estimate given below (18). If the micro-conductors are too small their orientation with the external field, necessary for field amplification, will be disrupted by Brownian motion. We can use the electrostatic energy (10) to estimate the magnitude of the thermal disruption of orientation: the difference in energy between a spheroid oriented with the field and one oriented at angle θ to the field has the magnitude

$$\Delta W = \tfrac{1}{2}\varepsilon {E_0}^2 (\alpha_\ell - \alpha_t) \sin^2\theta \tag{20}$$

We have inserted the dielectric constant ε of the medium into (20), as noted below equation (13). Thermal motion at absolute temperature T will produce misalignment from the field direction given by equating (20) to the thermal energy ½kT associated with one degree of freedom (in this case of rotation about an axis perpendicular to the electric field).

For blood at 37 °C (310 K), with $\varepsilon \approx 80$, external electric field strength 2 MV m^{-1}, and $c = 1\,\mu$m, equating (20) to ½kT gives $\theta \approx 1$ mrad. At this field strength, thermal disruption of the spheroidal micro-conductors is negligible provided the larger semi-axis c is substantially larger than about 10 nm (this value of c gives $\varepsilon {E_0}^2 (\alpha_\ell - \alpha_t) \approx kT$).

Table 1 gives representative rotation times Ω^{-1} and upper and lower limits on semi-major axis values c for external fields ranging from 0.2–2 MV m^{-1} (2–20 kV cm^{-1}). The Ω^{-1} values are obtained from (17) with $F(e)$ approximated by unity (compare figure 4), and with the viscosity of blood at 37 °C. The estimates of largest permissible c values which keep the Reynolds number below unity is obtained by setting (18) less than or equal to unity, which restricts the

Table 1. Representative rotation times Ω^{-1} and upper and lower limits on semi-major axis values c for external fields ranging from 0.2–2 MV m^{-1} (2–20 kV cm^{-1}).

External field	0.2	0.5	1	2	E_0 (V μm^{-1})
Rotation time	250	40	10	2.5	Ω^{-1}(μs)
Largest c	30	12	6	3	c_{max} (μm)
Smallest c	95	52	33	20	c_{min} (nm)

product $E_0 c$ to be less than 6 V. The lower limit on c comes from limiting the thermal disruption of the orientation of the micro-conductors. We set the electrostatic energy ten time greater than the thermal energy, $\varepsilon {E_0}^2 (\alpha_\ell - \alpha_t) \approx 10kT$, and take the c/a ratio to be 15.7 (to give a field amplification factor of 100 at the spheroid ends); for this aspect ratio $\alpha_\ell - \alpha_t \approx 0.13c^3$ from (14). From the Table we see that, at 2 MV m^{-1}, any spheroidal conductor semi-axis size from about 20 nm to a few microns would be suitable for enhancement of electroporation.

A Reviewer has suggested that the Joule heating in the micro-conductors also needs to be estimated. It turns out to be negligible, as the following rough argument shows. The dipole moment p may be approximated for elongated spheroids as $2cQ$, c being the longer semi-axis, and $+Q$, $-Q$ the charges near each end. The current I is dQ/dt, and gives the Joule heating I^2R, where R is the spheroid resistance to internal current flow. For iron spheroids with $c = 1$ micron and aspect ratio 15.69, R is about 15 Ω. By taking a cycle average for an oscillatory external field (angular frequency ω), one obtains the Joule heating per cycle. When the spheroid is nearly aligned with the external field, the operative polarizability is the longitudinal one, so the dipole moment p is nearly equal to the longitudinal polarizability times the electric field. The dominant dimensional factors in the ratio of the Joule heating per cycle to the electrostatic orientation energy given by (20) are $\omega\rho 4\pi\varepsilon_0$. The resistivity ρ for iron is about $10^{-7}\,\Omega\,\mathrm{m} = 10^{-7}\,\mathrm{s\,m\,F^{-1}}$, and $4\pi\varepsilon_0$ is about $10^{-10}\,\mathrm{F\,m^{-1}}$. Thus the $\rho 4\pi\varepsilon_0$ product is about 10^{-17} s, and hundreds of billions of cycles at megahertz frequency would be needed to make the total Joule heating comparable to the electrostatic orientation energy.

6. Discussion

We have investigated a form of electroporation cancer therapy, in which the electric field is enhanced by injection of internal micro-conductors together with anticancer drugs. To this end, we have studied the field amplification at a conducting prolate spheroid, the torque acting on the spheroid at arbitrary orientation due to the external field (which always tries to align it with the field), the viscous forces retarding its rotation, and also the thermal disruption of the orientation of the optimal orientation.

The model of prolate spheroids in a viscous medium is clearly a great simplification of the reality. However, the author believes that it can be useful to have exact results (in the present case for the field amplification, torque due to field and retarding torque due to viscous drag) as bench marks, even if they are necessarily for idealized situations. A worker in electroporation can at least know precisely what the field amplification and torques are for a given aspect ratio of a prolate spheroid, for example. To illustrate this point, consider equation (1) of (Rojas-Chapana *et al* 2004), which estimates the field enhancement at the end of a straight nanotube to be 3 times its length divided by its diameter. [An average value is surely intended, because the field near the end of a nanotube varies rapidly with position.] For a prolate spheroid this estimate would give $3c/a$ (correct in the spherical limit), whereas the exact formula (8) gives, for c large compared to a,

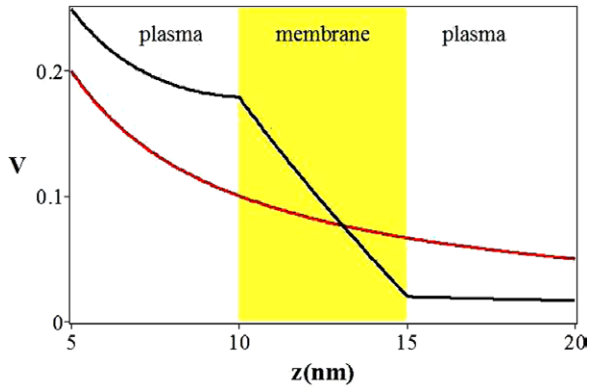

Figure 5. The potential of a point charge (at the origin, to the left of the diagram), outside and inside a membrane of 5 nm thickness. The membrane face nearer the charge is at separation 10 nm from the charge. The potential shown is along the line normal to the membrane and passing through the charge. The smooth curve shows what the potential would be in the absence of the membrane.

$$\frac{E_p}{E_0} = \frac{(c/a)^2}{\ln\frac{2c}{a} - 1} - \frac{1}{4}\frac{6\ln\frac{2c}{a} - 5}{\left[\ln\frac{2c}{a} - 1\right]^2} + O(a/c)^2 \tag{21}$$

The first term of (21) gives a field magnification of 100.654 when $c/a = 15.69164$ (100 is the exact value), whereas the approximation $3c/a$ is both analytically and numerically incorrect.

A point raised by a Reviewer is that the field amplification factor will be different in the the neighbourhood of a cell membrane (lipid bilayer). The field surrounding a spheroid which is near a cell wall is difficult to calculate. However, since the micron-sized spheroids are large compared to the thickness of the cell membrane (about 5 nm), the situation where one end of the spheroid is close to the cell can be approximated by that of a point charge near a planar cell membrane, discussed in the Appendix. Figure 5 shows the electric potential outside and inside a membrane 5 nm thick, when the charge is 10 nm away from the left side of the membrane. The dielectric constants of the plasma and cytoplasm (outside and inside the cell) and of the membrane are taken to be $\varepsilon_p \approx 80, \varepsilon_m \approx 2$ (Gabriel *et al* 1996, Markx and Davey 1999, Sudsiri *et al* 2007). The membrane dielectric value is at the low end of estimated values, so the effect of the membrane as shown in figure 5 is the largest possible, as the dielectric contrast between membrane and plasma or cytoplasm assumes its largest quoted value. The field just inside the membrane is larger than that just outside by the factor $\varepsilon_p / \varepsilon_m \approx 40$ (at both boundaries), because of the continuity of εE at the interface. Note that the electric field (the slope of the potential curve) is nearly constant inside the membrane in the case illustrated; for a uniform external field it would be constant, inside and outside.

Of course the tissue surrounding cancer cells, unless blood, is generally is not well approximated by a viscous fluid. There will be elastic response to deformation in general. This is much harder to estimate, but one can say that the rotation of micro-electrodes will be more impeded than by viscosity alone. Therefore the calculations given provide an upper limit on the rotation rates, and also on the thermal motion of the micro-electrodes.

Taking an aspect ratio such that the field amplification at the sharp ends of the spheroid is by a factor of 100 when the spheroid is oriented along the field, a possible range of the long

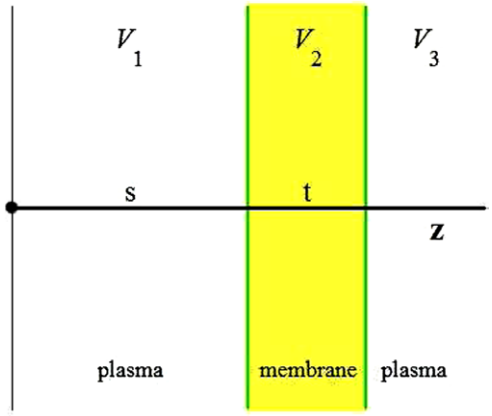

Figure 6. A point charge Q (at the origin of coordinates), separated by distance s from the near side of a planar membrane, which is of thickness t. The dielectric constant on either side of the membrane is ε_p; inside the membrane it is ε_m .

semi-axis lengths for the conducting spheroids is 0.02–3 microns, assuming a fluid medium with the viscosity of blood and an external field of 2 MV m^{-1}.

It will clearly be advantageous for the patient if the injected micro-electrodes are biodegradable and as small as practicable (within the ranges given in table 1). Sub-micron iron spheroids may be removed quickly enough by oxidation. Another possibility is the use of electrospun conductive polypyrrole nanofibres (Chronakis *et al* 2006, Lee *et al* 2009), which can be made largely biodegradable as polypyrrole-polylactide conductors (Shi *et al* 2008).

The author (a physics theorist) hopes that an *in vitro* trial will test the proposal presented here.

Acknowledgement

This paper has benefited from constructive comments and suggestions of the reviewers.

Appendix: point charge near a dielectric plate

This problem is solved in full generality by Smythe (Smythe 1950, section 5.303), but the potential involves infinite integrals over Bessel functions which are lengthy to evaluate numerically. We shall give a closed-form solution for the potential along the line perpendicular to the membrane passing through the charge, namely along the z-axis in figure 6.

Smythe gives only the potential $V_3(r,z)$ explicitly; we shall state them all for completeness:

$$\frac{\varepsilon_p V_1(r,z)}{Q} = \frac{1}{(r^2+z^2)^{\frac{1}{2}}} - \chi \int_0^\infty \mathrm{d}k\, J_0(kr)\, \frac{\mathrm{e}^{k(z-2s)}[1-\mathrm{e}^{-2kt}]}{1-\chi^2\mathrm{e}^{-2kt}} \tag{A1}$$

$$\frac{\varepsilon_p V_2(r,z)}{Q} = (1-\chi) \int_0^\infty \mathrm{d}k\, J_0(kr)\, \frac{\mathrm{e}^{-kz}+\chi\mathrm{e}^{k(z-2s-2t)}}{1-\chi^2\mathrm{e}^{-2kt}} \tag{A2}$$

$$\frac{\varepsilon_p V_3(r,z)}{Q} = \int_0^\infty \mathrm{d}k\, J_0(kr)\, \frac{(1-\chi^2)\,\mathrm{e}^{-kz}}{1-\chi^2\mathrm{e}^{-2kt}} \tag{A3}$$

Here $r^2 = x^2 + y^2 : r$ is the distance from the z-axis. The quantity χ is given by

$$\chi = \frac{\varepsilon_m - \varepsilon_p}{\varepsilon_m + \varepsilon_p} \tag{A4}$$

Along the z-axis ($r = 0$) the expansion

$$[1 - \chi^2 \mathrm{e}^{-2kt}]^{-1} = \sum_{n=0}^{\infty} \chi^{2n} \mathrm{e}^{-2nkt} \tag{A5}$$

and integration over k reduces all the integrals to infinite sums. For example (we restrict ourselves to the region $z>0$ throughout),

$$\frac{\varepsilon_p V_3(0,z)}{Q} = (1-\chi^2) \sum_{n=0}^{\infty} \frac{\chi^{2n}}{2nt+z} \tag{A6}$$

If we write $S(t,z,\chi)$ for the sum in (A6), differentiation with respect to χ leads to the partial differential equation

$$\partial_\chi S + \chi^{-1} \frac{z}{t} S = (t\chi)^{-1} (1-\chi^2)^{-1} \tag{A7}$$

The solution of (A7) satisfying the condition $S(t,z,0) = z^{-1}$ is

$$S(t,z,\chi) = \frac{1}{z} F\left(1, \frac{z}{2t}; 1 + \frac{z}{2t}; \chi^2\right) \tag{A8}$$

where F is the hypergeometric function. All of the potentials can be expressed in terms of S:

$$\frac{\varepsilon_p V_1(0,z)}{Q} = \frac{1}{z} - \chi [S(t, 2s-z, \chi) - S(t, 2s+2t-z, \chi)\ ] \tag{A9}$$

$$\frac{\varepsilon_p V_2(0,z)}{Q} = (1-\chi)\ [S(t,z,\chi) - \chi S(t, 2s+2t-z, \chi)\ ] \tag{A10}$$

$$\frac{\varepsilon_p V_3(0,z)}{Q} = (1-\chi^2)\, S(t,z,\chi) \tag{A11}$$

The electric fields are given by $E_z = -\partial_z V$ in each of the three regions. At the boundaries we have the ratio $\varepsilon_p / \varepsilon_m$ between the fields:

$$\varepsilon_p E_z^{(1)}(s) = \varepsilon_m E_z^{(2)}(s)\,, \qquad \varepsilon_m E_z^{(2)}(s+t) = \varepsilon_p E_z^{(3)}(s+t) \tag{A12}$$

Of course, the equalities (A12) are incorporated into the solution as the continuity of the normal value of the displacement at the boundaries. As the charge approaches the membrane the field just outside the membrane tends to $1 + \chi = 2\varepsilon_m / (\varepsilon_p + \varepsilon_m)$ times the field that would be there in the absence of the membrane. The field just inside the membrane is larger than that outside by the factor $\varepsilon_p / \varepsilon_m$, as always.

References

Batchelor G K 1970 Slender body theory for particles of arbitrary cross-section in Stokes flow *J. Fluid Mech.* **44** 419–40

Chen C, Evans J A, Robinson M P, Smye S W and O'Toole P 2008 Measurement of the efficiency of cell membrane electroporation using pulsed ac fields *Phys. Med. Biol.* **53** 4747–57

Chen C, Evans J A, Robinson M P, Smye S W and O'Toole P 2010 Electroporation of cells using EM induction of pulsed ac fields by a magnetic stimulator *Phys. Med. Biol.* **55** 1219–29
Chronakis I S, Grapenson S and Jakob A 2006 Conductive polypyrrole nanofibers via electrospinning: electrical and morphological properties *Polymer* **47** 1597–603
Edwardes D 1892 Steady motion of a viscous fluid in which an ellipsoid is constrained to rotate about a principal axis *Quart. J. Pure Appl. Math.* **26** 70–8
Gabriel C, Gabriel S and Corthout E 1996 The dielectric properties of biological tissues: I. Literature survey *Phys. Med. Biol.* **41** 2231–49
Gans R 1928 Zur theorie der Brownschen molekularbewegung *Ann. Phys.* **391** 628–56
Gaynor P T and Bodger P S 2006 Physical modelling of electroporation in close cell-to-cell proximity environments *Phys. Med. Biol.* **51** 3175–88
Gothelf A, Mir L M and Gehl J 2003 Electrochemotherapy: results of cancer treatment using enhanced delivery of bleomycin by electroporation *Cancer Treat. Rev.* **29** 371–87
Granot Y, Ivorra A, Maor E and Rubinsky B 2009 *In vivo* imaging of irreversible electroporation by means of electrical impedance tomography *Phys. Med. Biol.* **54** 4927–43
Hoffmann G A, Dev S B, Dimmer S and Nanda G S 1999 Electroporation therapy: a new approach for the treatment of head and neck cancer *IEEE Trans. Biomed. Eng.* **46** 752–9
Ivorra A, Al-Sakere B, Rubinsky B and Mir L M 2009 *In vivo* electrical conductivity measurements during and after tumor electroporation: conductivity changes reflect the treatment outcome *Phys. Med. Biol.* **54** 5949–63
Landau L D and Lifshitz E M 1960 *Electrodynamics of Continuous Media* (Pergamon: Oxford)
Lee J Y, Bashur C A, Goldstein A S and Schmidt C E 2009 Polypyrrole-coated electrospun PLGA nanofibers for neural tissue applications *Biomaterials* **30** 4325–35
Levine Z A and Vernier P T 2010 Life cycle of an electropore: field-dependent and field-independent steps in pore creation and annihilation *J. Membrane Biol.* **236** 27–36
Markx G H and Davey C L 1999 The dielectric properties of biological cells at radiofrequencies: applications in biotechnology *Enzyme Microb. Technol.* **25** 161–71
Mir L M 2000 Therapeutic perspectives of *in vivo* cell electropermeabilization *Bioelectrochemistry* **53** 1–10
Morse P M and Feshbach H 1953 *Methods of Theoretical Physics* (New York: McGraw-Hill)
Pliquett U, Joshi R P, Sridhara V and Schoenbach K H 2007 High electrical field effects on cell membranes *Bioelectrochemistry* **70** 275–82
Raffa V *et al* 2011 Carbon nanotube-mediated wireless cell permeabilization: drug and gene uptake *Nanomedicine* **6** 1709–18
Raffa V, Ciofani G and Cuschieri A 2009 Enhanced low voltage cell electropermeabilization by boron nitride nanotubes *Nanotechnology* **20** 075104
Raffa V, Ciofani G, Vittorio O, Pensabene V and Cuschieri A 2010a Carbon nanotube-enhanced cell electropermeabilization *Bioelectrochemistry* **79** 136–41
Raffa V, Ciofani G, Vittorio O, Pensabene V and Cuschieri A 2010b Physicochemical properties affecting cellular uptake of carbon nanotubes *Nanomedicine* **5** 89–97
Rojas-Chapana J S, Correa-Duarte M A, Ren Z, Kempa K and Giersig M 2004 Enhanced introduction of gold nanoparticles into vital acidothiobacillus ferrooxidans by carbon nanotube-based microwave electroporation *Nano Lett.* **4** 985–8
Sersa G, Miklavcic D, Cemazar M, Rudolf Z, Pucihar G and Snoj M 2008 Electrochemotherapy in treatment of tumours *EJSO* **34** 232–40
Shi G, Zhang Z and Rouabhia M 2008 The regulation of cell functions electrically using biodegradable polypyrrole-polylactide conductors *Biomaterials* **29** 3792–8
Shine A D and Armstrong R C 1987 The rotation of a suspended axisymmetric ellipsoid in a magnetic field *Rheol. Acta* **26** 152–61
Smythe W R 1950 *Static and Dynamic Electricity* (New York: McGraw-Hill)
Sudsiri J, Wachner D and Gimsa J 2007 On the temperature dependence of the dielectric properties oh human red blood cells *Bioelectrochemistry* **70** 134–40
Vernier P T, Sun Y and Gundersen M A 2006 Nanoelectropulse-driven membrane perturbation and small molecule permeabilization *BMC Cell Biol.* **7** 37
Weaver J C and Chimadzhev Y A 1996 Theory of electroporation: a review *Bioelectrochem. Bioenerg.* **41** 135–60